Scientia Iranica F (2019) 26(3), 1980–1989

Sharif University of Technology
Scientia Iranica
Transactions F: Nanotechnology
http://scientiairanica.sharif.edu

Ti6Al4V coating with B_2O_3 and Al_2O_3 containing hydroxyapatite by HVOF technique

A. Evcin* **and B. Büyükleblebici**

Department of Materials Science and Engineering, Faculty of Engineering, University of Afyon Kocatepe, 03200 Afyon, Turkey.

Received 21 May 2018; received in revised form 11 October 2018; accepted 12 January 2019

KEYWORDS
Bioceramics;
Hydroxyapatite;
Implant;
Sol-gel;
Coating;
HVOF.

Abstract. Calcium phosphates (Ca-P) based bioceramics have proved to be alluring materials for biomedical applications. Among them, hydroxyapatite (HA), $Ca_{10}(PO_4)_6(OH)_2$, is the most frequently used bioceramic. Due to its favorable properties and biocompatibility, HA-coated Ti6Al4V alloy has become one of the most interesting implant materials for orthopedic and dental applications. High-Velocity Oxy Fuel (HVOF) is a method employed to coat metallic implants such as titanium (Ti) and its alloy (Ti6Al4V) with hydroxyapatite (HA). In this study, decreasing the crack occurrence and increasing adhesion strength were investigated. For this purpose, nano sized HA, alumina (Al_2O_3) doped HA, and Boron oxide (B_2O_3) doped HA powders were produced by sol-gel process. First, a series of HA/Al_2O_3, HA/B_2O_3 coatings were deposited on Ti6Al4V substrate by HVOF method. Powders were tested by Fourier-Transform Infrared (FTIR) and X-Ray Diffraction (XRD). Morphology of specimens was characterized by Scanning Electron Microscopy (SEM-EDX). Adhesion strength of specimens was found to be affected by increase in the amounts of Al_2O_3 and B_2O_3 in HA. Furthermore, water contact angles of surface were decreased with increase in the amounts of Al_2O_3 and B_2O_3 in HA. This coating surface was expected to combine the advantages of Ca-P application and improve adhesion strength.

1. Introduction

Biomaterials are described as natural or synthetic materials that are used in human body and materials to evaluate, support, or replace any tissue or organ [1]. They can be classified into the traditional categories of metals, ceramics, polymers, and composites. Metallic biomaterials like Co-Cr-Mo alloys, 316L stainless steel, and Ti and Ti alloys have found application in orthopedics [2-4].

The success of biomaterials depends on physical and mechanical properties as well as biocompatibility. Biocompatibility is a term that describes acceptance of implant by the surrounding tissue and organ. It is the chemical and/or physical interaction between materials and body fluids, and determines how much the physiological consequences of this interaction are damaging to the body. The biocompatibility of a material is identified by means of in vivo and/or in vitro tests. In vitro tests, to mimic the environment in which it will have to survive, the material is exposed to Simulated Body Fluids (SBFs) [5].

CaPs, in particular hydroxyapatite (HA), are often used in the coating of metals to offer the biocompatibility and mechanical strength of both types of materials. The thickness of HA coating is very important [6,7]. Teng et al. studied Sr-substituted hydroxyapatite (Sr-HA) coatings on Ti metal. They found out that bioactivity of the Sr-HA coatings was

*. *Corresponding author. Tel.: +90-272-2281423; Fax: +90-272-2281422*
E-mail address: evcin@aku.edu.tr (A. Evcin); bakileblebici@hotmail.com (B. Büyükleblebici)

doi: 10.24200/sci.2019.50994.1958

significantly better than that of uncoated Titanium [8]. Furko et al. created multi-element modified HA bioceramics coating on Ti6Al4V by Ag, Zn, Mg, Sr ions [9]. Kitsugi et al. stated that mechanical properties and biocompatibility of the B_2O_3 modified Apatite-Wollastonite (A-W) were comparable with those of A-W ceramics [10]. Park showed the effect of the amount of Al_2O_3 in A-W on bone bonding strength [11]. Afzal et al. concluded that HA- Al_2O_3-YSZ was produced by spark plasma sintering [12]. Evcin et al. identified the effect of ZrO_2 and Al_2O_3 in HA bioceramics on mechanical properties [13]. B_2O_3 is a fluxing agent at high temperature because of its low melting point (450°C); it is used to decrease sintering temperature for ceramics. Harabi et al. studied the addition of B_2O_3 to dental ceramics. They observed that addition of 3 and 5 wt.% B_2O_3 decreased the sintering temperature by 25°C and 50°C, respectively [14]. Wu et al. produced hydroxyapatite/Al_2O_3 on titanium using a multi-step technique. They found out that HA/Al_2O_3 coating on Ti improved both adhesive strength and biocompatibility [15].

While many metals and their alloys meet many biomechanical requirements of orthopedic implants, their biocompatibility is lower than that of ceramic biomaterials. For this reason, calcium phosphates, such as HA, have been used as coating on metallic implants. The methods of HA coating for biomedical applications are given in Table 1.

HVOF coating is a thermal spray coating method used in production of metallic coating [1]. HVOF is a high-energy thermal spray process. This method produces dense and strong coatings and gives perfect performance in aggressive, wear, and corrosive environments [32]. Evcin and Bohur showed the effect of silica in HA on chemical structure and morphological properties [33]. Melero et al. studied plasma sprayed HA coatings for biomedical purposes. They obtained composite coatings by HVOF spray [34]. The flame can be supplied by using acetylene, hydrogen, natural gas, or hydrocarbon fuels. HVOF is a process with high performance, low cost, and acceptable coating-substrate adhesion. Figure 1 shows the fundamentals of HVOF method. Heating source is the fuel and the powder is carried through carrier gases [35,36].

In the present study, nano-size HA powders with Al_2O_3 and B_2O_3 as additives were prepared. Then, HVOF method was used to coat Ti6Al4V substrates with HA; our aim was to investigate the presence manner of Al_2O_3 and B_2O_3 in the HA and their effects on mechanical surface properties and biocompatibility.

2. Materials and method

To synthesize powders chemically, analytic-grade $Ca(NO_3)_2$, $(NH_4)_2HPO_4$, NH_4OH, $Al(OC_3H_7)_3$, IPA,

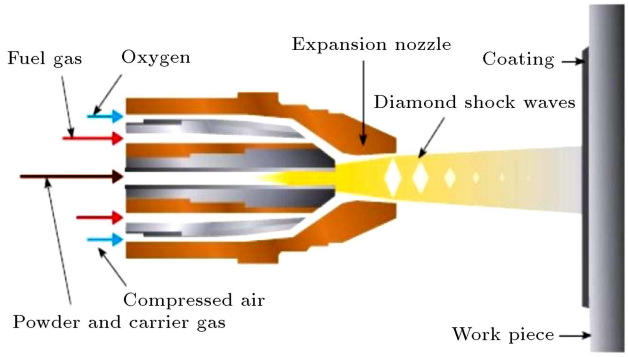

Figure 1. Schematic diagram of the HVOF coating process.

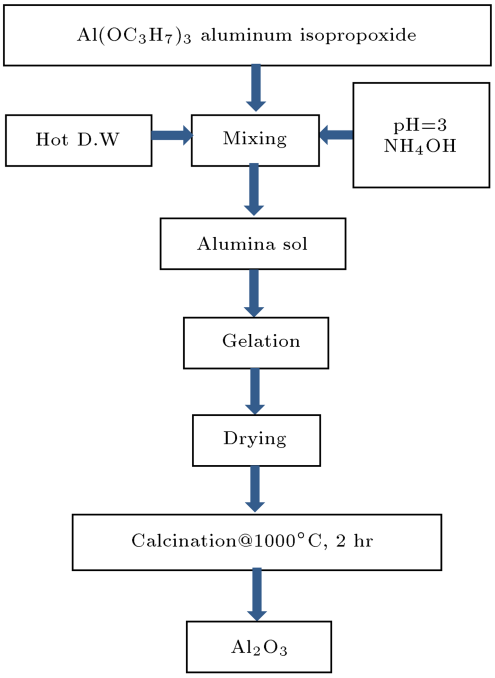

Figure 2. Al_2O_3 production by sol-gel method.

and $B(OC_3H_7)_3$ were used as precursors. All chemicals were purchased from Merck and used as received. Ti6Al4V was used as metallic implant for coating. First, Al_2O_3 and B_2O_3 were synthesized by sol-gel process (Figures 2 and 3). Al_2O_3 and B_2O_3 doped HA powders were also prepared in the same route with the ratios of 1, 2, and 3 wt% (Figure 4).

The FTIR spectra of Al_2O_3 and B_2O_3 doped hydroxyapatite were studied by means of Perkin-Elmer 460 Spectrums BXI spectrometer. Crystal structures of pure HA, and Al_2O_3 and B_2O_3 doped HA powders were analysed by XRD (Bruker D 8 Advance) using Cu-Kα X-rays at the wavelength of 1.5406 Å (2θ range: 20-90°, step size: 0.1972°). Scratch test was performed by using a Rockwell C diamond indenter. The indenter was spherical (200 μm radius). It was slid over the metallic surface and the load changed from 0.05 to 30 N

Table 1. Comparison of different methods for HA coating.

Technique	Thickness (μm)	Advantages	Disadvantages	Reference
Thermal spray	30-200	Higher density Higher hardness Low price Possibility of Automation	Over-spray High consumption of material amorphous structure	[16]
Sputter coating	0.5-3	Uniform thickness Dense coating Better adhesion	Line-of-sight process Slow deposition rate Amorphous structure	[17]
Electron-beam deposition	1	Uniform thickness High deposition rate	Line-of-sight process Non-uniform evaporation rate Amorphous structure	[18]
Dip coating	50-500	Simultaneous coating of top and bottom Inexpensive No waste of material	Coating of both surfaces Big volume, much solution Not applicable to prismatic and cubic shapes	[19]
Electrophoretic deposition	0.1-2.0	Uniform thickness High deposition rates Complex substrates	High sintering temperatures Crack-defects	[20]
Hot isostatic pressing	0.2-2.0	Improving mechanical and physical properties Near net shape Full density	Expensive High temperature Cycle times can be slow	[21]
Biomimetic coating	< 30	Safety Simplicity Applicability to a large variety of materials	Weak adhesion Resorbability The use of high temperature	[22]
Pulsed laser deposition	$\sim$ 0.05-10	Large variety of material Good adhesion Controlling the stoichiometric ratio	Small target size Expensive High substrate temperature Defects in the substrate surface	[23]
Dynamic mixing	0.05-1.3	High adhesive strength	Amorphous structure	[24]
Sol-gel	< 1	Less energy consumption Better homogeneity Low cost Very thin films	Cost of precursors Shrinkage Difficulty in avoiding residual porosity and OH groups	[25]

Table 1. Comparison of different methods for HA coating (continued).

Technique	Thickness (μm)	Advantages	Disadvantages	Reference
Ion beam-assisted deposition	$\sim$ 0.03-4	Inexpensive Dense pore-free coating Microstructure control High surface quality Dense smooth films	Line-of-sight process Amorphous structure	[26]
Powder Plasma Spray (PPS)	$\sim$ 30-300	Higher quality coatings Many types of substrate material Micro-rough surface and porosity	High temperature Rapid cooling produces crack Non-uniform thickness Very expensive Poor control of biodegragation	[27]
Liquid plasma spray (LPS) and Suspension Plasma spray (SPS)	$\sim$ 5-50	High density True composition Very fine porosity Microstructure control	Line-of-sight process Expensive High temperature Non-uniform thickness	[28]
RF magnetron sputtering	$\sim$ 0.04-3.5	Better film quality Deposition of a wide variety of materials Operating at low pressures Uniform thickness	Line-of-sight process Expensive power supply Non-uniform thickness Very low deposition rate	[29]
Electrochemical deposition	< 95	Low processing temperature Complex shape coating Control of thickness of the coating Good composition Microstructure control	Costly Time-consuming	[30]
Plasma Electrolytic Oxidation (PEO) or micro arc oxidation	< 100	Corrosion resistance Good mechanical properties Oxidation resistance Thermal resistance	Al, Mg, and Ti and their alloys	[31]

at a speed of 29.95 N/mm according to standard testing methods.

Thickness of coating layer was obtained from the cross-sectional images using a scanning electron microscope (LEO 1430 VP). Surface roughness of the coating surfaces was identified in a contact mode by using a surface profilometer (Mitutoyo Surftest SJ-210). Each sample was measured 5 times at selected locations and an average surface roughness was measured. Contact angle measurements with SBF solution were performed using KSV Attention Theta Lite Tensiometer.

Coating with pure and Al_2O_3/B_2O_3 doped HAs was carried out through HVOF process at Kuantamet Limited, Ankara, Turkey. Ti6Al4V alloy (ASTM F-1472) was used as the substrate material (Figure 5). All specimens to be coated were grit blasted with alumina

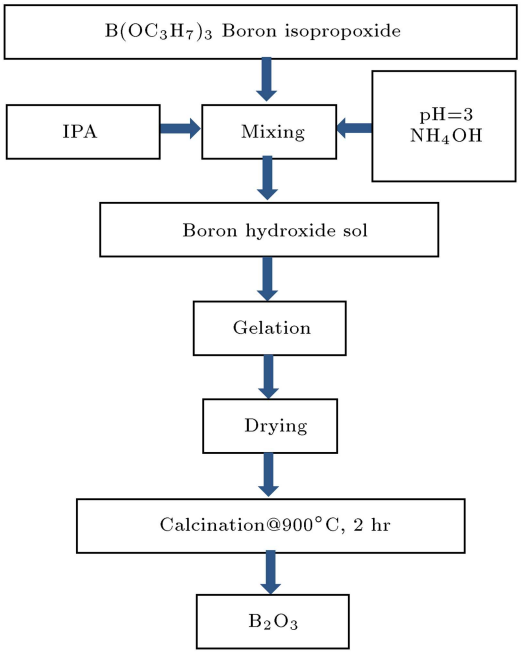

Figure 3. B_2O_3 production by sol-gel method.

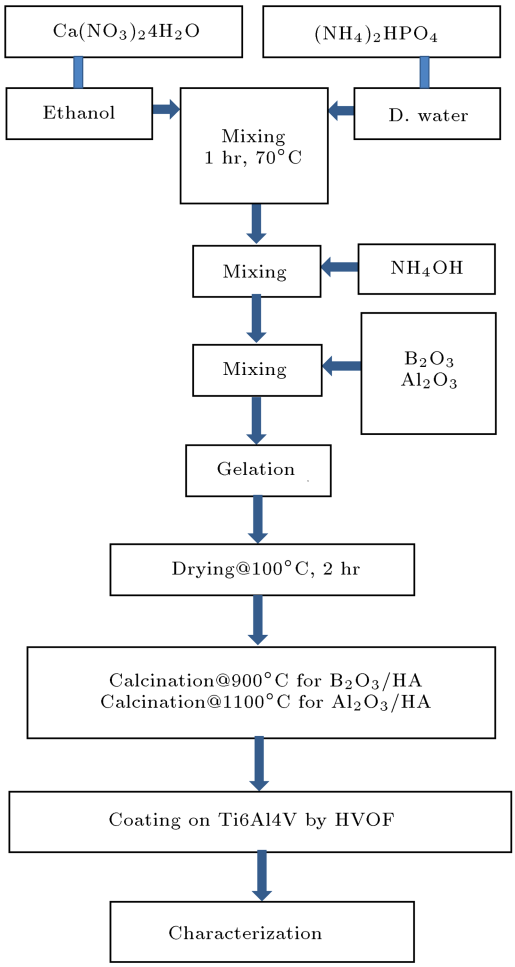

Figure 4. Flow chart of the sol-gel procedure and HVOF coating.

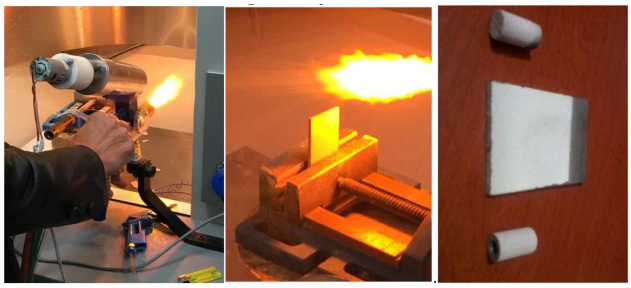

Figure 5. HVOF coating of samples and coated Ti6Al4V implants.

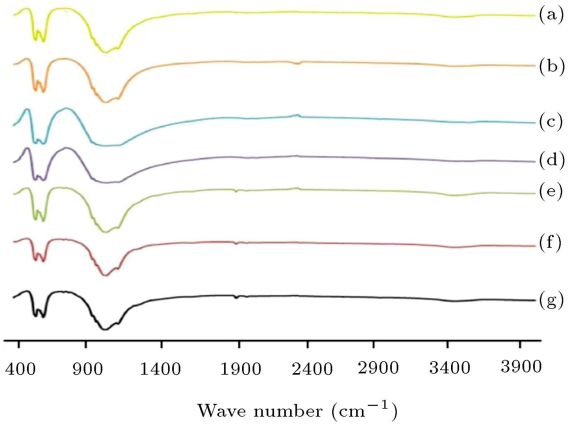

Figure 6. FTIR spectra of pure and doped HA: (a) Pure HA, (b) 1% Al_2O_3, (c) 2% Al_2O_3, (d) 3% Al_2O_3, (e) 1% B_2O_3, (f) 2% B_2O_3, and (g) 3% B_2O_3.

Table 2. HVOF parameters.

HVOF parameter	Setting
Coating distance (mm)	250
Coating time (sn)	20-30
Propan gas pressure (bar)	1
Oxygen gas pressure (bar)	2.3
Coating temperature (°C)	2000

(60-80 μm) at 0.44 MPa. Specifications of HVOF coating are given below in Table 2.

3. Result and discussion

The infrared spectrum (Figure 6) shows all kinds of characteristic peaks for pure and doped hydroxyapatites. Figure 6 shows the PO_4^{3-} bands at 1100, 1040, 960, 600, and 560 cm^{-1} [37]. This demonstrates that all specimens have retained the HA structure. FTIR analysis was performed to prove the functional groups and to check the formation of boron-related bands, BO_3^{3-} and BO_2^-, in the doped HA structure. The bands at 1250 cm^{-1} and 770 cm^{-1} are for the antisymmetric stretching and the symmetric bending modes of the

BO_3^{3-} groups, respectively; the bands at 2005 and 1930 cm^{-1} are related to the antisymmetric stretching of BO_2^- groups; the band at 3570 cm^{-1} is attributed to the stretching mode of hydroxyl group; and the peak at 810 cm^{-1} is for the vibration mode of Al-O bonds [38].

XRD patterns of pure HA, and Al_2O_3 and B_2O_3 doped HAs are shown in Figure 7. The figure shows

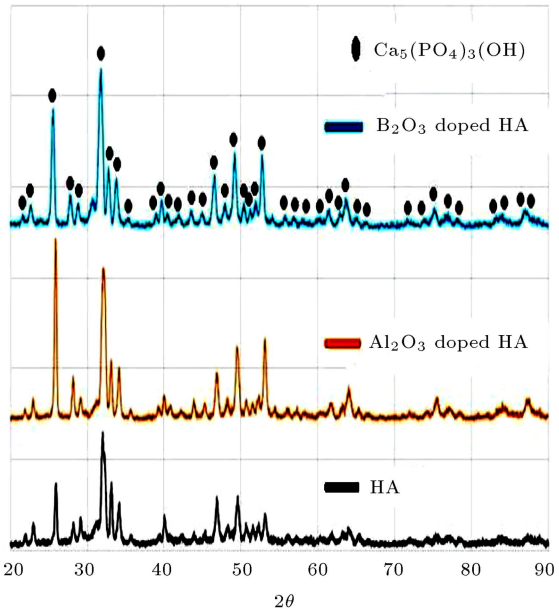

Figure 7. XRD patterns of pure-HA, 3 wt% Al_2O_3-doped HA and B_2O_3-doped HA.

that all the samples exhibit characteristic peaks for HA [39]. These patterns very well match the standard JCPDS database of HA (PDF No: 09-0432). The peaks of Al_2O_3 and B_2O_3 doped HAs show no significant difference from that of pure HA. No secondary phases, such as tricalcium phosphate (TCP) and precursor materials, were detected in these samples [40]. In fact, the XRD patterns indicate that the Al_2O_3 and B_2O_3 doping did not change the phase composition of the HA [41].

Images of the Rockwell C indentations are shown in Figure 8. It can be seen that the load led to radial plastic deformation of the HA coating.

As it can be seen in Figure 8, HA-coated Ti6Al4V leads to more deformation at the edge and more delamination than the Al_2O_3/Ti6Al4V and B_2O_3/Ti6Al4V samples do. In addition, when percentage of Al_2O_3 and B_2O_3 increases, scratch resistance of coating also increases.

Thickness of coating layer is given in Figure 9. When the amount of Al_2O_3 in HA increases, thickness of coating also increases. Coatings with average thickness between 71 and 157 μm were obtained in this work. The thickness of the coatings significantly decreases with increase in the amount of B_2O_3.

As shown in Figure 10, surface roughness of coating increases with increase in the amount of Al_2O_3 and B_2O_3. Average surface roughness is 10.4 μm for Al_2O_3 comprising HA coating and 8.3 μm for B_2O_3 comprising HA coating.

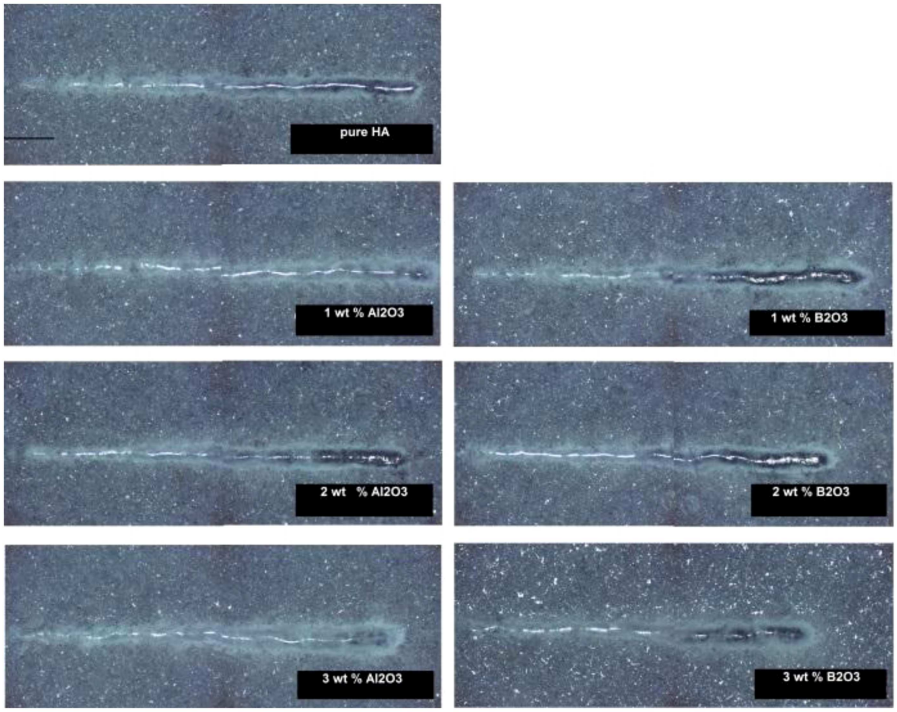

Figure 8. Scratch tracks of coatings.

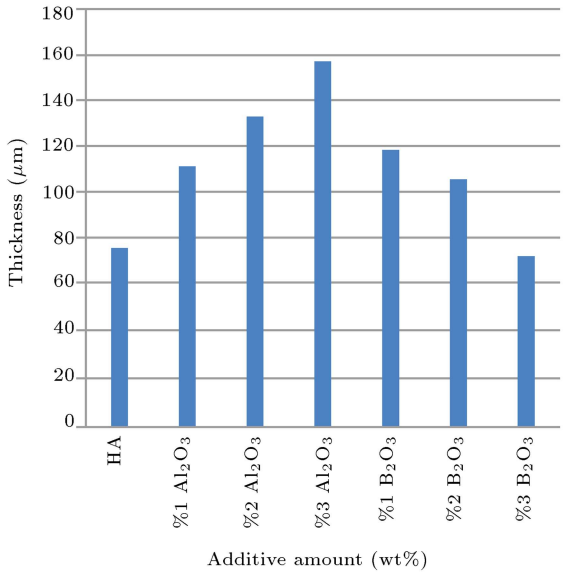

Figure 9. Coating thickness as a function of additive amount (wt%).

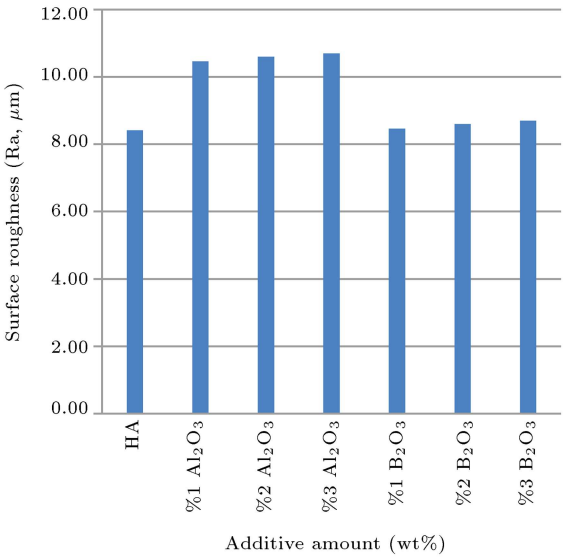

Figure 10. Surface roughness as a function of additive amount (wt%).

Pure HA coated implant has hydrophobic character. With increase in the amounts of Al_2O_3 and B_2O_3, Contact Angles (CA) of coatings decrease (Figure 11 and Table 3) and the coating layer tends to more hydrophobic character. Low CA ($< 90°$) corresponds to hydrophilic surface and high CA ($> 90°$) represents hydrophobic surface. It is also noteworthy that the bacteria adhere to materials with varying hydrophobicity, which depends on the hydrophobic properties of both material surface and the bacteria [9].

The biocompatibility of the specimens was tested by using SBF solution. SBF solution was synthesized based on the method suggested by Kokubo et al. [42].

Table 3. Contact angles (CA, degree) of samples.

Sample	CA (L)	CA (R)	Mean
Ti-6Al-4V (without grinding)	70.8	69.1	70.0
Ti-6Al-4V (surface ground)	67.8	73.8	70.8
Pure HA	105.8	107.1	106.5
%1 Al_2O_3 doped HA	92.0	91.8	92.0
%2 Al_2O_3 doped HA	94.4	96.8	95.6
%3 Al_2O_3 doped HA	79.7	82.5	81.1
%1 B_2O_3 doped HA	90.1	87.7	89.0
%2 B_2O_3 doped HA	64.0	63.4	63.7
%3 B_2O_3 doped HA	31.2	43.9	37.6

Coated Ti implant samples were immersed for 4, 7, 14, and 21 days in SBF solution. Then, samples were weighed and characterized by SEM. Hydroxyapatite nucleation in SBF solutions is usually utilized to determine the bioactivity of implants. After each dipping, the specimen was removed from the SBF and then, dried in ambient temperature. It is clear that the weight of samples changed after 4 days of immersion. Hydroxyapatite nucleation on surface was observed by SEM-EDX (Figure 12). The results show that the amount of particles formed on the Al_2O_3/HA and B_2O_3/HA coated Ti6Al4V implant increased with increase in soaking time. EDX results confirmed that the new crystal structure was HA (CA/P=20.94/12.27=1.71). It had the very similar ratio of Ca/P=1,67.

4. Conclusion

In this study, we demonstrated that Al_2O_3 and B_2O_3 doped HA composite powders could be used as coating on Ti6Al4V by HVOF technique. The obtained coating layer had approximately 100 μm thickness. Bioactivity results showed that Al_2O_3/HA coated Ti6Al4V implant was more bioactive than B_2O_3/HA coated Ti6Al4V implant. This was confirmed by the weight assessment and SEM images. Both HA coated layers had scratch resistance. Al_2O_3/HA coated Ti6Al4V implant offered higher scratch resistance than B_2O_3/HA coated Ti6Al4V implant did. The average surface roughness was around 10 μm for Al_2O_3/HA coated Ti6Al4V implant and around 8 μm for B_2O_3/HA coated Ti6Al4V implant. Al_2O_3 and B_2O_3 containing HA coatings exhibited hydrophilicity, whereas pure HA coatings were found to be hydrophobic. The observations of this study can be useful in biomedical applications of implant. In particular, the protective metal oxide

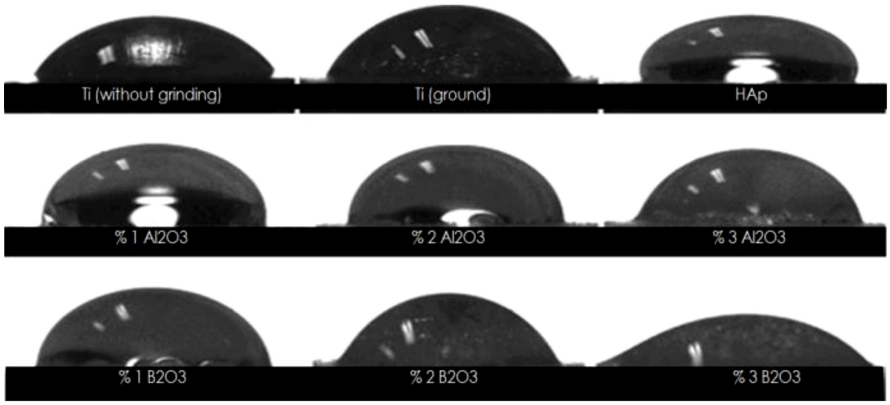

Figure 11. Contact angles of coating.

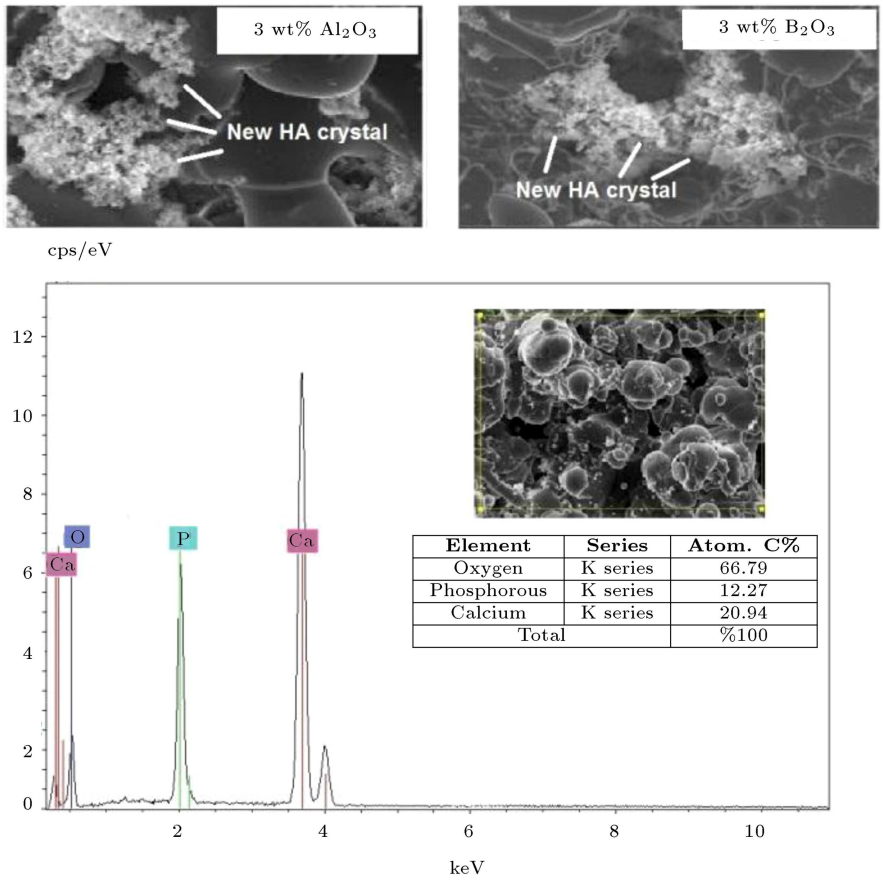

Element	Series	Atom. C%
Oxygen	K series	66.79
Phosphorous	K series	12.27
Calcium	K series	20.94
Total		%100

Figure 12. SEM images and EDX results for the surface after soaking SBF (21 days).

surfaces produced by HVOF method provide important insights into the future design of hybrid biomaterials in orthopedic treatments.

Acknowledgement

This study was supported by the Afyon Kocatepe University Scientific Research Projects Coordination Unit (Grand number 14.FEN.BİL.41).

References

1. Si, D., *Introduction to Biomaterials*, Tsinghua University Press, China (2005).
2. Nakai, M., Niinomi, M., Hieda, J., Yilmazer, H., and Todaka, Y. "Heterogeneous grain refinement of biomedical Ti-29Nb-13Ta-4.6Zr alloy through high-pressure torsion", *Sci. Iran. Trans. F*, **20**(3), pp. 1067-1070 (2013).
3. Okulov, I.V., Okulov, A.V., Soldatov, I.V., Luthringer,

B., Willumeit-Römer, R., Wada, T., Kato, H., Weissmüller, J., and Markmann, J. "Open porous dealloying-based biomaterials as a novel biomaterial platform", *Mater. Sci. Eng. C*, **88**, pp. 95-103 (2018).

4. Jin, W. and Chu, P.K. "Surface functionalization of biomaterials by plasma and ion beam", *Surf. Coat. Technol.*, **336**, pp. 2-8 (2018).

5. Wen, C., *Surface Coating and Modification of Metallic Biomaterials*, Elsevier, UK (2015).

6. Gozalian, A., Behnamghader, A., Daliri, M., and Moshkforoush, A. "Synthesis and thermal behavior of Mg-doped calcium phosphate nanopowders via the sol gel method", *Sci. Iran. Trans. F*, **18**(6), pp. 1614-1622 (2011).

7. Shahi, S., and Karbasi, S. "Evaluation of physical and mechanical properties of B-tri-calcium phosphate/poly-3-hydroxybutyrate nanocomposite scaffold for bone tissue engineering application", *Sci. Iran.*, **24**(3), pp. 1654-1668 (2017).

8. Teng, H.P., Lin, H.Y., Huang, Y.H., and Lu, F.H., "Formation of strontium-substituted hydroxyapatite coatings on bulk Ti and TiN-coated substrates by plasma electrolytic oxidation", *Surf. Coat. Technol.*, **350**, pp. 1112-1119 (2018).

9. Furko, M., Havasi, V., Kónya, Z., Grünewald, A., Detsch, R., Boccaccini, A.R., and Balázsi, C. "Development and characterization of multi-element doped hydroxyapatite bioceramic coatings on metallic implants for orthopedic applications", *Bol. Soc. Esp. Ceram. Vidr*, **57**(2), pp. 55-65 (2018).

10. Kitsugi, T., Nakamura, T., Yamamuro, T., Kokubo, T., Shinbuya, T., and Takagi, T. "SEM-EPMA observation of three types of apatite-containing glass-ceramics implanted in bone: the variance of a Ca-P-rich layer", *J. Biomed. Mater. Res.*, **21**, pp. 1255-1271 (1987).

11. Park, J. and Ozturk, A. "Bioactivity of apatite-wollastonite glass-ceramics produced by melt casting", *Surf. Rev. Lett.*, **20**(1), pp. 1350010-1350017 (2013).

12. Afzal, M.A.F., Kesarwani, P., Reddy, K.M., Kalmodia, S., Basu, B., and Balani, K. "Functionally graded hydroxyapatite-alumina-zirconia biocomposite: Synergy of toughness and biocompatibility", *Mater. Sci. Eng. C*, **32**(5), pp. 1164-1173 (2012).

13. Evcin, A., Coşkun, S., and ve Koyaş, S. "The production and characterization of bioceramic powders incorporated by ZrO_2 and Al_2O_3", *12th International Materials Symposium*, 15-17 October 2008, Pamukkale University, Denizli, pp. 1380-1386 (2008).

14. Harabi, A., Guerfa, F., Harabi, E., Benhassine, M.T., Foughali, L., and Zaiou, S. "Preparation and characterization of new dental porcelains, using K-feldspar and quartz raw materials. Effect of B2O3 additions on sintering and mechanical properties", *Mater. Sci. Eng. C*, **65**(1), pp. 33-42 (2016).

15. Wu, Z.J., He, L.P., and Chen, Z.Z. "Fabrication and characterization of hydroxyapatite/Al_2O_3 biocomposite coating on titanium", *Trans Nonferrous Met. Soc. China*, **16**(2), pp. 259-266 (2006).

16. Günen, A. "Micro-abrasion wear behavior of thermal-spray-coated steel tooth drill bits", *Acta Phys. Pol. A*, **130**, p. 217 (2016).

17. Park, S.Y. and Choe, H.C. "Mn-coatings on the micropore formed Ti-29Nb-xHf alloys by RF-magnetron sputtering for dental applications", *Appl. Surf. Sci.*, **432**, B, pp. 278-284 (2018).

18. Hristu, R., Stanciu, S.G., Tranca, D.E., and Stanciu G.A. "Electron beam influence on the carbon contamination of electron irradiated hydroxyapatite thin films", *Appl. Surf. Sci.*, **346**, pp. 342-347 (2015).

19. Trujillo, C.D., Peón, E., Chicardi, E., Pérez, H., and Torres, Y. "Sol-gel deposition of hydroxyapatite coatings on porous titanium for biomedical applications", *Surf. Coat. Technol.*, **333**, pp. 158-162 (2018).

20. Rad, M.F. "Effect of morphology on the electrophoretic deposition of hydroxyapatite nanoparticles", *J. Alloys Compd.*, **741**, pp. 211-222 (2018).

21. Suresh, M.B., Biswas, P., Mahender, V., and Johnson, R. "Comparative evaluation of electrical conductivity of hydroxyapatite ceramics densified through ramp and hold, spark plasma and post sinter Hot Isostatic Pressing routes", *Mater. Sci. Eng. C*, **70**(1), pp. 364-370 (2017).

22. Shen, S., Cai, S., Bao, X., Xu, P., and Xu, G. "Biomimetic fluoridated hydroxyapatite coating with micron/nano-topography on magnesium alloy for orthopaedic application", *Chem. Eng. J.*, **339**, pp. 7-13 (2018).

23. Wang, D.G., Chen, C.Z., Yang, X.X., Ming, X.C., and Zhang, W.L. "Effect of bioglass addition on the properties of HA/BG composite films fabricated by pulsed laser deposition", *Ceram. Int.*, **44**(12), pp. 14528-14533 (2018).

24. Yoshinari, M., Ohtsuka, Y., and Dérand, T. "Thin hydroxyapatite coating produced by the ion beam dynamic mixing method", *Biomaterials*, **15**(7), pp. 529-535 (1994).

25. Gharazi, S., Ershad-Langroudi, A., and Rahimi, A. "The influence of silica synthesis on the morphology of hydrophilic nanocomposite coating", *Sci Iran, Trans F*, **18**(3), pp. 785-789 (2011).

26. Rabiei, A., Thomas, B., Jin, C., Narayan, R., Cuomo, J., Yang, Y., and Ong J.L. "A study on functionally graded HA coatings processed using ion beam assisted deposition with in situ heat treatment", *Surf. Coat. Technol*, **200**(20-21), pp. 6111-6116 (2006).

27. Pillai, R.S., Frasnelli, M., and Sglavo, V.M. "HA/β-TCP plasma sprayed coatings on Ti substrate for biomedical applications", *Ceram. Int.*, **44**(2), pp. 1328-1333 (2018).

28. Candidato Jr., R.T., Sokołowski, P., Pawłowski L., Nana G.L., Constantinescu C., Denoirjean A. "Development of hydroxyapatite coatings by solution precursor plasma spray process and their microstructural Characterization", *Surf. Coat. Technol*, **318**, pp. 39-49 (2017).

29. Surmenev, R.A., Surmeneva, M.A., Grubova, I.Y., Chernozem, R.V., and Epple M. "RF magnetron sputtering of a hydroxyapatite target: A comparison study on polytetrafluorethylene and titanium substrates", *Appl. Surf. Sci.*, **414**, pp. 335-344 (2017).

30. Chen, Z., Liu, Y., Mao, L., Gong, L., Sun, W., and Feng L. "Effect of cation doping on the structure of hydroxyapatite and the mechanism of defluoridation", *Ceram. Int.*, **44**, pp. 6002-6009 (2018).

31. Barooghi, B., Sheikhi, M., and Amiri, A. "Effect of processing time on microstructure of surface and corrosion resistance of coatings resulted by plasma electrolytic oxidation on titanium alloy in hydroxyapatite nano-particles electrolyte", *Sci Iran, Articles in Press, Accepted Manuscript* , Available Online from 24 Sep. 2018.

32. Kulpetchdara, K., Limpichaipanit, A., Rujijanagul, G., Randorn, C., and Chokethawai K. "Influence of the nano hydroxyapatite powder on thermally sprayed HA coatings onto stainless steel", *Surf. Coat. Technol.*, **306**, Part A, pp. 181-186 (2016).

33. Evcin, A. and Bohur, B. "Coating of different silica sources containing hydroxyapatite for Ti6Al4V metal substrate using HVOF technique", *4th International Conference on Computational and Experimental Science and Engineering (ICCESEN-2017)*, Antalya-Turkey, p. 726 (2017).

34. Melero, H., Fargas, G., Garcia-Giralt, N., Fernández J., and Guilemany, J.M. "Mechanical performance of bioceramic coatings obtained by high-velocity oxy-fuel spray for biomedical purposes", *Surf. Coat. Technol.*, **42**, pp. 92-9915 (2014).

35. Kawakita, J., Kuroda, S., Fukushima, T., and Kodama, T. "Development of dense corrosion resistant coatings by an improved HVOF spraying process", *Science and Technology of Advanced Materials*, **4**(4), pp. 281-289 (2003).

36. Yadaw, R.C., Singh, S.K., Chattopadhyaya, S., Kumar S., and Singh R.C. "Tribological behavior of thin film coating-a review", *International Journal of Engineering & Technology*, **7**(3), pp. 1656-1663 (2018).

37. Wang, D.G., Ming, X.C., Zhang, W.L., Zhang, J.H., Chen, C.Z. "Effect of heat treatment on the properties of HA/BG composite films", *Ceram. Int.*, **44**(6), pp. 7228-7233 (2018).

38. Albayrak, Ö. "Structural and mechanical characterization of boron doped biphasic calcium phosphate produced by wet chemical method and subsequent thermal treatment", *Mater Charact*, **113**, pp. 82-89 (2016).

39. Khaleghpanah, S., Abachi, P., and Dolati, A. "The effect of current density on microstructural homogeneity, hardness, fracture toughness and electrochemical behavior of electrodeposited Cu-0.5Co/WC nanocomposite coating", *Sci. Iran.*, **24**(6), pp. 3505-3511 (2017).

40. Yuan, Q., Xu, A., Zhang, Z., Chen, Z., Wan, L., Shi, X., Lin, S., Yuan, Z., Deng, L. "Bioactive silver doped hydroxyapatite composite coatings on metal substrates: Synthesis and characterization", *Mater. Chem. Phys.*, **218**, pp. 130-139 (2018).

41. Baradaran, S., Tabrizi, B.N., Shirazi, F.S., Samandari, S.S., Shahtalebi, S., and Basirun, W.J. "Wet chemistry approach to the preparation of tantalum-doped hydroxyapatite: Dopant content effects", *Ceram Int.*, **44**(3), pp. 2768-2781 (2018).

42. Kokubo, T., Kushitani, H., Sakka, S., Kitsugi, T., and Yamamuro, T. "Solutions able to reproduce in vivo surface-structure changes in bioactive glass-ceramic A-W", *J. Biomed. Mater. Res.*, **24**, pp. 721-734 (1990).

Biographies

Atilla Evcin is an Associate Professor in Materials Science & Engineering at the University of Kocatepe, where he has been a faculty member since 1994. He was Engineering Faculty's vice dean. Since 2016, he has been the head of the Department of Nanoscience and Nanotechnology. Dr. Evcin completed his PhD at Sakarya University and his undergraduate studies at Anadolu University. His research interests lie in the areas of nanomaterials, biomaterials, and sol-gel processing, coating, and surface modification. He has collaborated actively with researchers in several other disciplines of science, particularly physics, chemistry, and biology. He has 30 SCI indexed articles, 97 international conference papers, 27 other indexed articles, and 47 conference papers.

Baki Büyükleblebici was born in Afyonkarahisar in 1988. He graduated from Cumhuriyet High School and began academic studies at Afyon Kocatepe University. After finishing academic studies, he has been working as Management Representative and Laboratory Supervisor in Tuğad Clay and Mine Co.